Electronic Supplementary Information (ESI) for

Pyrite (FeS_2) Nanocrystals as Inexpensive High-Performance Lithium-Ion Cathode and Sodium-Ion Anode Material

by Marc Walter, [†,‡] Tanja Zünd, [†,‡] and Maksym V. Kovalenko*[†,‡]

[†] Laboratory of Inorganic Chemistry, Department of Chemistry and Applied Biosciences, ETH Zürich, CH-8093 Zürich, Switzerland

[‡] Laboratory for Thin Films and Photovoltaics, Empa – Swiss Federal Laboratories for Materials Science and Technology, CH-8600 Dübendorf, Switzerland

[*]E-mail: mvkovalenko@ethz.ch

Materials and Methods.

Synthesis of FeS_2 NCs. FeS_2 NCs were synthesized by a modified procedure of the synthesis published by Li *et al.*[1] $FeCl_2$ (6.7 mmol, 99.5%, abcr) was added to oleylamine (160 mL, 80-90%, Acros) and the mixture was kept for 1 hour at 100 ^oC under vacuum. Then the flask was set under nitrogen, the temperature was increased to 120 ^oC and elemental sulfur (40 mmol, 99.998%, Sigma-Aldrich) previously dissolved in oleylamine (40 mL) was injected. The resulting black reaction mixture was subsequently heated to 220 ^oC and kept at this temperature for two hours. After two hours the reaction mixture was cooled to room temperature and the resulting material was washed with chloroform and ethanol. Typically, 0.8 g of FeS_2 NCs were obtained using this procedure corresponding to a relative yield of ca. 99%. The main difference to the procedure of Li *et al.* is in the upscaling of all quantities by a factor of 16. Further, the injection of the S-oleylamine solution was carried out at 120 ^oC, not at 100 ^oC, in order to obtain all FeS_2 NCs in 50-100 nm size range. [For comparison, at 100 ^oC Li *et al.* have obtained sizes of 150-250 nm] As shown by the characterization of FeS_2 NCs in Figure 1 neither phase purity, morphology or size distribution is impaired by this modified procedure compared to the original work of Li *et al.*

Ligand removal. Oleylamine was removed from the surface of the NCs by hydrazine treatment. FeS_2 NCs were stirred for 2 hours in a solution of hydrazine (0.8 mL, GHC Gerling, Holz+Co) in anhydrous acetonitrile (25 mL, 99.8%, Sigma-Aldrich). Afterwards the material was washed three times with acetonitrile and dried under vacuum at room temperature.

Electrode fabrication, cell assembly and electrochemical measurements. The following battery components were used: carbon black (Super C65, TIMCAL), carboxymethyl cellulose (CMC, Grade: 2200, Daicel Fine Chem Ltd.), $NaClO_4$ (98%, Alfa Aesar, additionally dried), propylene carbonate (BASF, battery grade), 4-fluoro-1,3-dioxolan-2-one (fluoroethylene carbonate, FEC, Hisunny Chemical Co., battery grade), 1M $LiPF_6$ in EC:DMC (1:1; Merck, battery grade), glass microfiber separator (GF/D, Whatman), Cu foil (9µm, MTI Corporation). For electrode preparation, the respective materials were mixed with deionized water to form a homogeneous slurry using a Fritsch Pulverisette 7 classic planetary mill operated at 500 rpm for 1 hour. Materials were mixed with the ratio FeS_2:CB:CMC=64%:21%:15%. The resulting slurries were coated onto Cu foil and dried at 80 °C for 12 hours under vacuum (loading of active material ~0.5 mg/cm^2, thickness ~15 µm). Electrochemical measurements were conducted in air tight coin-type cells assembled in an Ar-filled glove box ($O_2 < 0.1$ ppm, $H_2O < 0.1$ ppm). Elemental lithium and sodium were employed as both reference and counter electrode in Li-ion half cells and Na-ion half cells respectively. As electrolyte 1M $LiPF_6$ in EC:DMC with 3% FEC was used for LIBs, whereas for SIBs 1M $NaClO_4$ PC with 10% FEC served as electrolyte. As separator glass fiber was used. Galvanostatic cycling tests were carried out at room temperature on MPG2 multi-channel workstation (BioLogic). Capacities were normalized by the mass of FeS_2.

Materials characterization. Transmission Electron Microscopy (TEM) images were obtained with a Philips CM30 TEM microscope at 300 kV using carbon-coated Cu grids as substrates (Ted-Pella). Scanning electron microscopy (SEM) was performed using a NanoSEM 230. Powder X-ray diffraction (XRD) was measured on a STOE STADI P powder X-ray diffractometer (Cu-Kα1 irradiation, $\lambda = 1.540598$ Å). Attenuated total reflectance Fourier transform infrared spectroscopy (ATR-FTIR) measurements were carried out on a Nicolet iS5 FT-IR spectrometer (Thermo Scientific). For *ex-situ* XRD measurements half-cells were transferred to and opened in an Ar-filled glovebox. The electrode material was removed carefully from the current collector and enclosed between two stripes of adhesive tape.

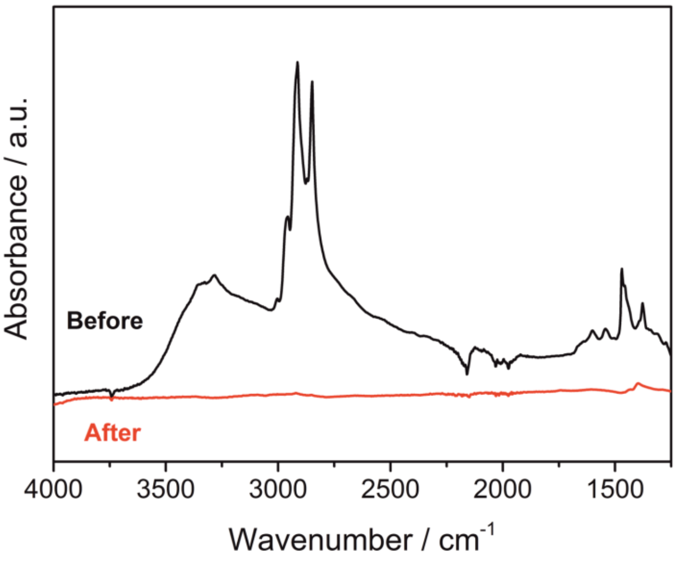

Figure S1. ATR-FTIR spectra of FeS_2 NCs before and after hydrazine treatment.

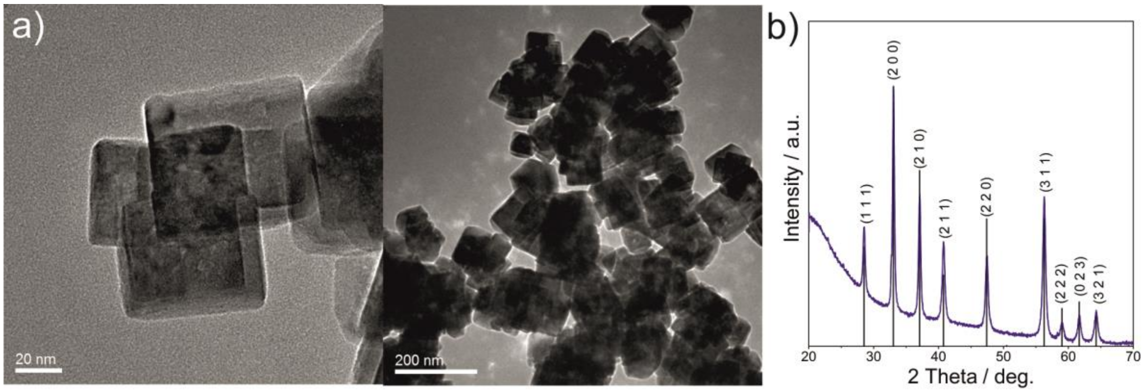

Figure S2. TEM-images (a) and XRD pattern (b) of FeS_2 NCs after hydrazine treatment.

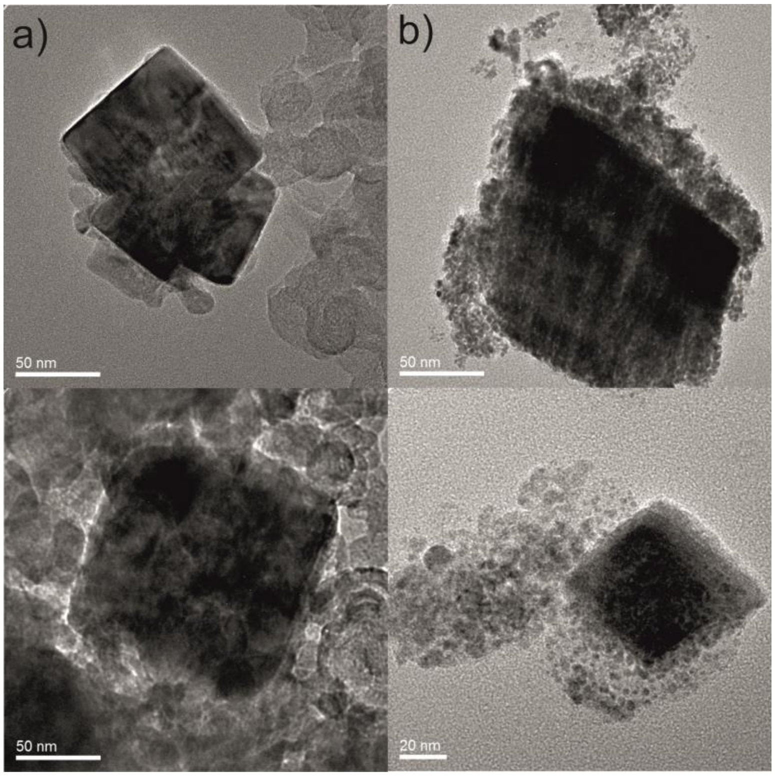

Figure S3. TEM-images of FeS_2 NC electrodes before (a) and after (b) 100 cycles of charge/discharge at a constant current of 1000 mAg^{-1} in the 0.02-2.5 V potential range in Na-ion half cells.

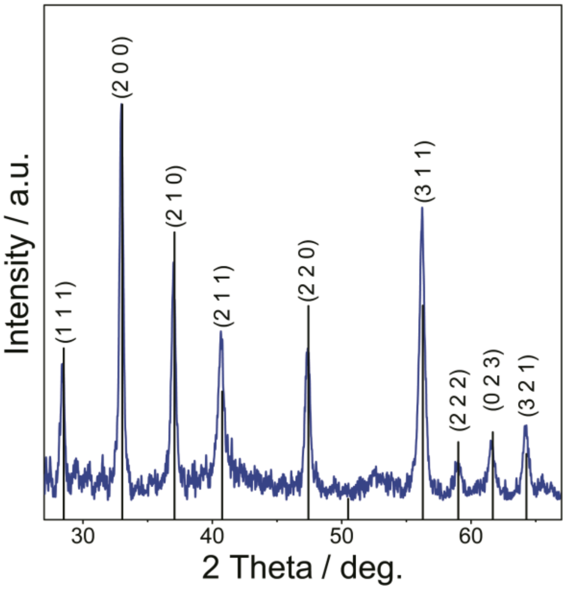

Figure S4. XRD pattern of FeS_2 NC electrodes before electrochemical cycling.

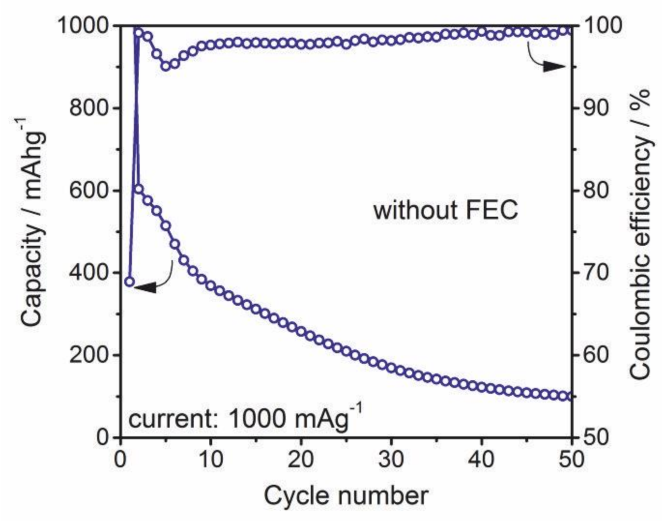

Figure S5. Capacity retention for FeS_2 NCs in Li-ion half cells without addition of FEC to the electrolyte. Cells were cycled in the potential range 1.0 – 3.0 V, except for the first discharge to 0.02 V.

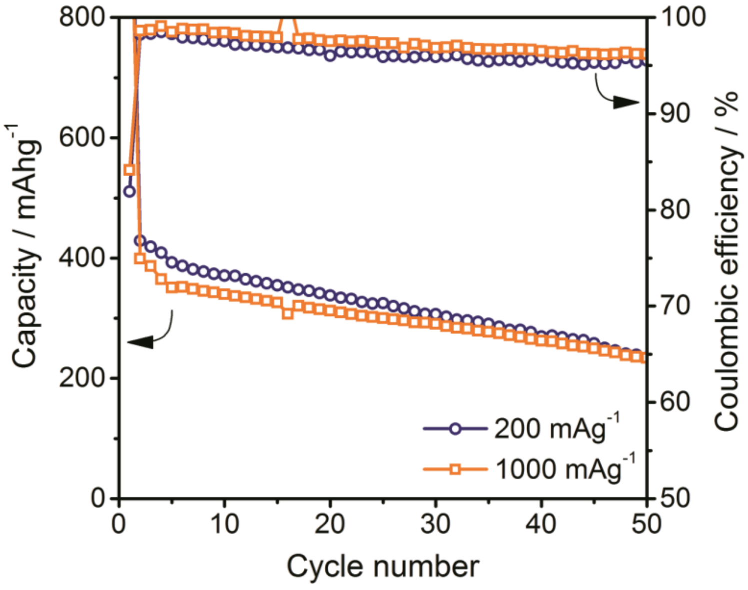

Figure S6. Capacity retention for FeS_2 NCs in Na-ion half cells. Cells were cycled in the potential range 1.0 – 3.0 V, except for the first discharge to 0.02 V.

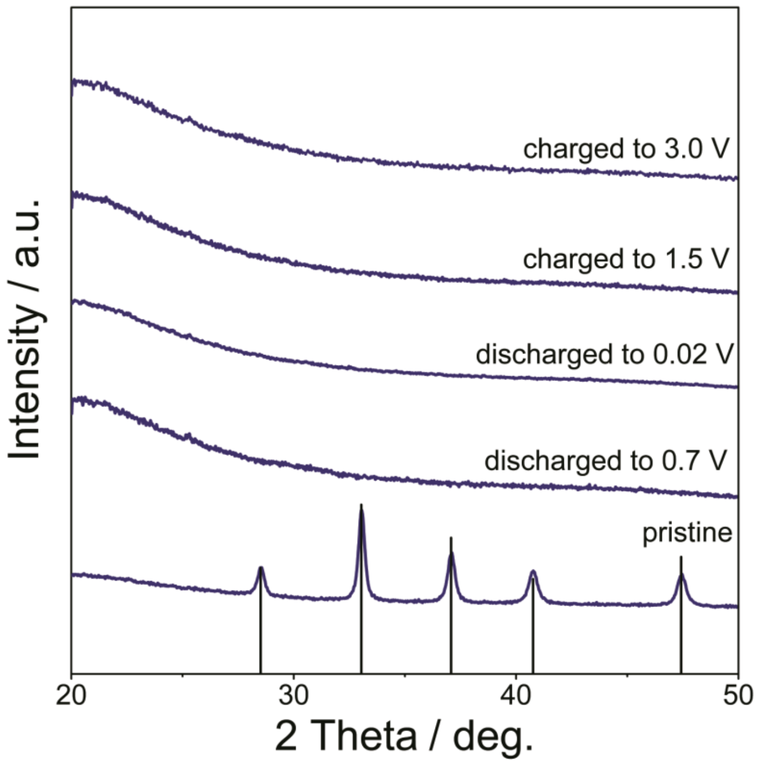

Figure S7. *Ex-situ* XRD measurements for the first discharge and charge cycle of FeS_2 NCs in Na-ion half cells. Cells were cycled with a current of 200 mAg^{-1}.

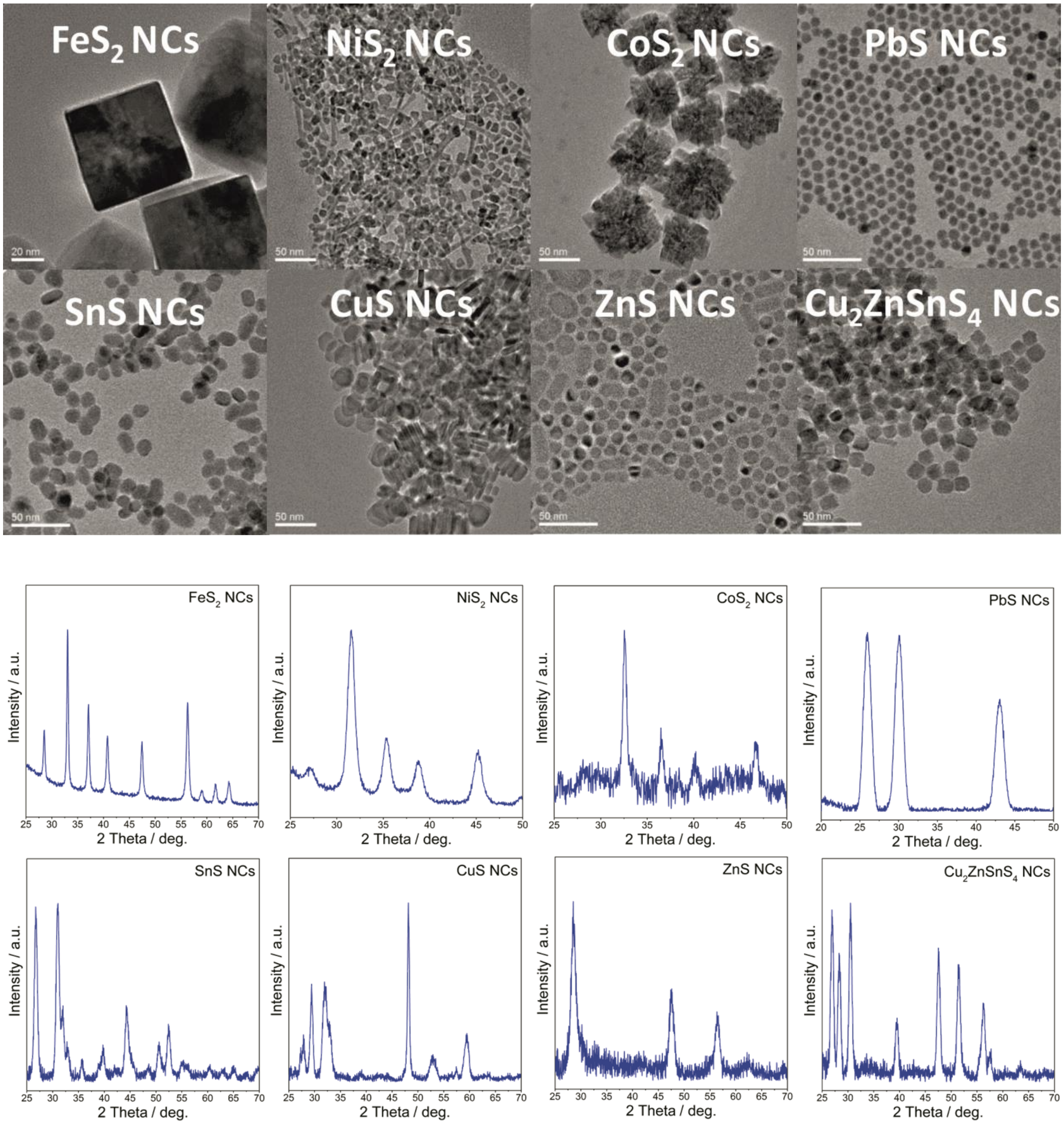

Figure S8. TEM-images and XRD patterns of various metal sulfide NCs synthesized according to known in the literature methods: *Nanotechnology* **2010**, *21*, 105707 (SnS), *Langmuir* **2005**, *21*, 9451 (CuS), *J. Am. Chem. Soc.* **2003**, *125*, 11100 (ZnS), *J. Am. Chem. Soc.* **2014**, *136*, 9236 (CZTS NCs). CoS_2 and NiS_2 NCs were synthesized analogously to FeS_2, but using $CoCl_2$ and $NiCl_2$ respectively instead of $FeCl_2$.

Table S1. Li-ion cathodic performance of FeS_2 NCs: Comparison of the electrochemical performance of the herein presented FeS_2 NCs with previously reported results by others.

Cathode	Current density	Initial capacity	Retained capacity	Cycle number	Reference
FeS_2 NCs	200 mAg^{-1}	800 $mAhg^{-1}$	720 $mAhg^{-1}$	50	Present work
	200 mAg^{-1}	800 $mAhg^{-1}$	630 $mAhg^{-1}$	100	
	1000 mAg^{-1}	800 $mAhg^{-1}$	600 $mAhg^{-1}$	50	
PAN-FeS_2	89.4 mAg^{-1}	729 $mAhg^{-1}$	470 $mAhg^{-1}$	50	[2]
submicron FeS_2	89.4 mAg^{-1}	~600 $mAhg^{-1}$	420 $mAhg^{-1}$	30	[3]
FeS_2 nanowires	89.4 mAg^{-1}	~400 $mAhg^{-1}$	350 $mAhg^{-1}$	50	[4]
FeS_2@C porous nanooctahedra	447 mAg^{-1}	550 $mAhg^{-1}$	495 $mAhg^{-1}$	50	[5]

Table S2. Na-ion cathodic performance of FeS_2 NCs: comparison of the electrochemical performance of the herein presented FeS_2 NCs with previously reported results by others.

Cathode	Current density	Initial capacity	Retained capacity	Cycle number	Reference
FeS_2 NCs	200 mAg^{-1}	430 $mAhg^{-1}$	240 $mAhg^{-1}$	50	Present work
	1000 mAg^{-1}	400 $mAhg^{-1}$	240 $mAhg^{-1}$	50	
FeS_2	40 mAg^{-1}	~500 $mAhg^{-1}$	~350 $mAhg^{-1}$	9	[6]
FeS_2	50 mAg^{-1}	~280 $mAhg^{-1}$	~70 $mAhg^{-1}$	50	[7]
FeS_2	50 mAg^{-1}	~450 $mAhg^{-1}$	~85 $mAhg^{-1}$	50	[8]

Table S3. Comparison of the electrochemical performance of the herein presented FeS_2 NCs with previously reported results obtained with metal sulfides as anode in SIBs.

Anode	Current density	Initial capacity	Retained capacity	Cycle number	Reference
FeS_2 NCs	1000 mAg^{-1}	820 $mAhg^{-1}$	606 $mAhg^{-1}$	200	Present work
	1000 mAg^{-1}	820 $mAhg^{-1}$	500 $mAhg^{-1}$	400	
	1000 mAg^{-1}	820 $mAhg^{-1}$	410 $mAhg^{-1}$	600	
	5000 mAg^{-1}	700 $mAhg^{-1}$	530 $mAhg^{-1}$	100	
MoS_2 nanosheets	20 mAg^{-1}	~160 $mAhg^{-1}$	~160 $mAhg^{-1}$	100	9
MoS_2/rGO	25 mAg^{-1}	~250 $mAhg^{-1}$	~220 $mAhg^{-1}$	25	10
MoS_2 nanoflowers	50 mAg^{-1}	~230 $mAhg^{-1}$	~350 $mAhg^{-1}$	300	11
	200 mAg^{-1}	~220 $mAhg^{-1}$	~310 $mAhg^{-1}$	600	
	1000 mAg^{-1}	~220 $mAhg^{-1}$	~300 $mAhg^{-1}$	1500	
nano MoS_2-C	1000 mAg^{-1}	854 $mAhg^{-1}$	484 $mAhg^{-1}$	100	12
nano TiO_2-MoS_2	100 mAg^{-1}	740 $mAhg^{-1}$	474 $mAhg^{-1}$	30	13
WS_2@graphene	20 mAg^{-1}	~584 $mAhg^{-1}$	329 $mAhg^{-1}$	500	13
SnS	125 mAg^{-1}	~520 $mAhg^{-1}$	370 $mAhg^{-1}$	30	14
Nano SnS-C	100 mAg^{-1}	486 $mAhg^{-1}$	548 $mAhg^{-1}$	80	15
SnS@graphene	810 mAg^{-1}	~500 $mAhg^{-1}$	492 $mAhg^{-1}$	250	16
SnS_2-rGO	1000 mAg^{-1}	594 $mAhg^{-1}$	500 $mAhg^{-1}$	400	17
rGO/Sb_2S_3	50 mAg^{-1}	670 $mAhg^{-1}$	~637 $mAhg^{-1}$	50	18

Supporting references:

1. W. Li, M. Doblinger, A. Vaneski, A. L. Rogach, F. Jackel and J. Feldmann, *J. Mater. Chem.*, 2011, **21**, 17946-17952.
2. S. B. Son, T. A. Yersak, D. M. Piper, S. C. Kim, C. S. Kang, J. S. Cho, S. S. Suh, Y. U. Kim, K. H. Oh and S. H. Lee, *Adv. Energy Mater.*, 2014, **4**.
3. D. Zhang, J. P. Tu, J. Y. Xiang, Y. Q. Qiao, X. H. Xia, X. L. Wang and C. D. Gu, *Electrochim. Acta*, 2011, **56**, 9980-9985.
4. L. Li, M. Caban-Acevedo, S. N. Girard and S. Jin, *Nanoscale*, 2014, **6**, 2112-2118.
5. J. Liu, Y. Wen, Y. Wang, P. A. van Aken, J. Maier and Y. Yu, *Adv. Mater.*, 2014, **26**, 6025-6030.
6. Z. Shadike, Y.-N. Zhou, F. Ding, L. Sang, K.-W. Nam, X.-Q. Yang and Z.-W. Fu, *J. Power Sources*, 2014, **260**, 72-76.
7. T. B. Kim, W. H. Jung, H. S. Ryu, K. W. Kim, J. H. Ahn, K. K. Cho, G. B. Cho, T. H. Nam, I. S. Ahn and H. J. Ahn, *J. Alloys Compd.*, 2008, **449**, 304-307.
8. T. B. Kim, J. W. Choi, H. S. Ryu, G. B. Cho, K. W. Kim, J. H. Ahn, K. K. Cho and H. J. Ahn, *J. Power Sources*, 2007, **174**, 1275-1278.
9. G. S. Bang, K. W. Nam, J. Y. Kim, J. Shin, J. W. Choi and S.-Y. Choi, *ACS Appl. Mater. Interfaces*, 2014, **6**, 7084-7089.
10. L. David, R. Bhandavat and G. Singh, *ACS Nano*, 2014, **8**, 1759-1770.
11. Z. Hu, L. Wang, K. Zhang, J. Wang, F. Cheng, Z. Tao and J. Chen, *Angew. Chem. Int. Ed.*, 2014, **53**, 12794-12798.
12. C. Zhu, X. Mu, P. A. van Aken, Y. Yu and J. Maier, *Angew. Chem. Int. Ed.*, 2014, **53**, 2152-2156.
13. W.-H. Ryu, J.-W. Jung, K. Park, S.-J. Kim and I.-D. Kim, *Nanoscale*, 2014, **6**, 10975-10981.
14. P. K. Dutta, U. K. Sen and S. Mitra, *RSC Adv.*, 2014, **4**, 43155-43159.
15. L. Wu, H. Lu, L. Xiao, J. Qian, X. Ai, H. Yang and Y. Cao, *J. Mater. Chem. A*, 2014, **2**, 16424-16428.
16. T. Zhou, W. K. Pang, C. Zhang, J. Yang, Z. Chen, H. K. Liu and Z. Guo, *ACS Nano*, 2014, **8**, 8323-8333.
17. B. Qu, C. Ma, G. Ji, C. Xu, J. Xu, Y. S. Meng, T. Wang and J. Y. Lee, *Adv. Mater.*, 2014, **26**, 3854-3859.
18. D. Y. W. Yu, P. V. Prikhodchenko, C. W. Mason, S. K. Batabyal, J. Gun, S. Sladkevich, A. G. Medvedev and O. Lev, *Nat. Commun.*, 2013, **4**, 2922.